Agricultural Water Management 201 (2018) 70–82

Contents lists available at ScienceDirect

Agricultural Water Management

journal homepage: www.elsevier.com/locate/agwat

Soil water and salinity dynamics under sprinkler irrigated almond exposed to a varied salinity stress at different growth stages

V. Phogat[a,b,*], T. Pitt[a], J.W. Cox[a,c], J. Šimůnek[d], M.A. Skewes[a]

[a] South Australian Research and Development Institute, GPO Box 397, Adelaide SA 5001, Australia
[b] CCS Haryana Agricultural University, Hisar 125004, India
[c] The University of Adelaide, PMB1 Glen Osmond SA 5064, Australia
[d] Department of Environmental Sciences, University of California, Riverside, CA 92521, USA

ARTICLE INFO

Keywords:
Almond
HYDRUS-2D
Salinity
Leaching
Water balance
Water use efficiency

ABSTRACT

Water use and salinity dynamics in the soils are the crucial management factors influencing the productivity and long-term sustainability of almond and associated environment. In this study, HYDRUS-2D was calibrated and validated on measured spatial and temporal water contents and soil salinities (EC_e) distributions under almond irrigated with different water qualities (EC_{iw}) at different physiological stages. During two irrigation seasons (2014–15 and 2015–16), less saline irrigation water (average EC_{iw} 0.78 dS/m) was substituted for recycled irrigation water (average EC_{iw} 1.9 dS/m) in three phenologically different growth stages; pre-pit hardening, kernel growth, and post-harvest, along with no and full substitution during the entire season. Graphical and statistical comparisons (RMSE, MAE, ME, the Nash and Sutcliffe model efficiency, and the coefficient of determination) between measured and simulated values of water contents and EC_e in the soil showed a close agreement in all treatments. The water balance data revealed that the seasonal crop evapotranspiration of almond (ET_c) varied from 850 to 955 mm in different treatments over the two seasons which represented 68–79% of the water application. Trees irrigated with only less saline water through the two seasons (average EC_{iw} 0.78 dS/m) showed 10% higher plant water uptake as compared to those irrigated with recycled water only (average EC_{iw} 1.9 dS/m). Substituting less saline irrigation during the kernel growth phase, between pit-hardening and harvest, showed greater water uptake by almond and lower salinity buildup in the soil as compared to treatments that substituted less saline irrigation early or late in the season. For all treatments, the average daily root zone EC_e (2.4–3.7 dS/m) remained above the level of the almond salinity tolerance threshold (EC_e = 1.5 dS/m) throughout the period of investigation. Water use efficiency of almonds varied in a narrow range (0.21–0.25 kg m^{-3}) for different treatments. Deep drainage below the root zone (2 m) varied from 22.4–31.1% of the total water application (Rainfall + Irrigation), which was episodic and insufficient to contain the salinity below the almond threshold. This study provided a greater understanding of soil water and salinity dynamics under almond irrigated with waters of varying qualities.

1. Introduction

Water is becoming increasingly scarce worldwide, and sustainable use of the available water resources is the major water policy challenge for the future. In water-stressed regions, strong constraints due to natural climatic variability and increased use by other users make the allocation of water the core challenge for water resource management (Alcon et al., 2013). In addition to issues related to water quantity, the quality of water plays an important role in the sustainability of irrigated lands, especially in the context of salinity build up that could adversely impact the agricultural/horticultural crop productivity (Bresler et al., 1982; Maas, 1990; Pitman and Laüchli, 2002; Assouline et al., 2015). Impacts of soil salinity are varied and highly influenced by the soil type, inherent layering and hydraulic heterogeneity, quality and quantity of irrigation, the method of irrigation, rainfall amounts and distribution patterns, and salt tolerance of crops. At the same time, the installation of highly efficient, partial cover, irrigation systems in high-value crops including almond has a narrow wetted area that tends to concentrate salts in the rootzone. During periods of water scarcity, when irrigators are forced to limit their leaching fractions or forced to apply groundwater/recycled water, salts can rapidly accumulate to dangerous levels.

Almond production in the arid and semi-arid regions of the world

* Corresponding author.
E-mail address: vinphogat@gmail.com (V. Phogat).

https://doi.org/10.1016/j.agwat.2018.01.018
Received 24 October 2017; Received in revised form 9 January 2018; Accepted 19 January 2018

remains vulnerable to water availability and soil salinity. Although almond is a drought tolerant tree (Torrecillas et al., 1996), its production and profitability are highly dependent on the supply of irrigation water. The adoption of efficient irrigation techniques can increase the production by as much as ten-fold compared to non-irrigated lands (Egea et al., 2010). On the other hand, almond is sensitive to salinity, having a production threshold with respect to the electrical conductivity of the soil saturation extract (EC_e) of 1.5 dS/m and a reduction in the growth rate of 19% for a unit increase in salinity beyond the threshold (Maas, 1990). Thus, the salinity levels higher than the threshold anytime during the cropping season can have a serious impact on growth and nut production. Therefore, proper irrigation management in the orchard is very important to obtain sustainable yield, leach harmful chemicals from the root zone, save precious water, and increase the shelf life of the fruits. Precise information on the salinity impact at different growth stages can help develop more robust orchard salinity management guidelines.

Different deficit irrigation options (regulated deficit irrigation, RDI; sustained deficit irrigation, SDI; and partial root zone drying, PRD), including their impact at different growth stages of almond (Girona et al., 2005; Goldhamer and Viveros, 2000; Romero et al., 2004; Goldhamer et al., 2006; Egea et al., 2010; Puerto et al., 2013) have been extensively studied over the almond growing season (Nortes et al., 2009; Egea et al., 2013; Monks et al., 2017). These investigations highlighted the impact of reduced water applications on various physiological parameters, kernel size, and kernel yield. Other studies focussed on the almond water requirement and crop coefficients (Stevens et al., 2012; Espadafor et al., 2015; García-Tejero et al., 2015), an irrigation system design (Phogat et al., 2012), and water productivity of almonds under reduced water applications (García-Tejero et al., 2011; Phogat et al., 2013). On the other hand, the studies on the implications of the application of saline/recycled water irrigation on the water availability to almonds and salinity dynamics in the soil are sparse. Notably, the salinity related studies are specifically focused on the identification of tolerant root stocks (Gradziel and Kester, 1998; Camposeo et al., 2011) and genotypes (Rouhi et al., 2007; Sorkheh et al., 2012; Rajabpoor et al., 2014; Bahrami et al., 2015). Franco et al. (2000) reported a 46% reduction in the almond kernels when seasonally irrigated with high salinity water (4.6 dS/m) compared to when less saline water (0.8 dS/m) was used. Nightingale et al. (1991) observed the greatest accumulation of salinity (5.7 dS/m) beneath the trickle line source for 50% ET_C irrigation and laterally away from the trickle line for 100 and 150% ET_C irrigation. Therefore, the information on the impact of saline/recycled water irrigation at different growth stages of almond on the water balance and salinity dynamics in the soil could improve the understanding of the use of such water for the almond production and ensure the long-term sustainability of high-value horticulture crops.

Predictive science and numerical models such as HYDRUS-2D (Šimůnek et al., 2016) present an excellent opportunity to gauge the impacts of irrigation practices (Kandelous and Šimůnek, 2010; Ramos et al., 2012; Phogat et al., 2012; González et al., 2015), water quality (Hassan et al., 2005; Ramos et al., 2011; Hassanli et al., 2016) and climate change (Austin et al., 2010) on potential water and salinity hazards and to control offsite movement of costly inputs into the surface and subsurface water bodies (Phogat et al., 2014). Moreover, the partial wetting pattern and irregular root water uptake in a drip-irrigated orchard make it difficult to apply and interpret standard water balance techniques and require a large number of measurements (Ben-Asher, 1979). Thus, a numerical model (HYDRUS-2D) was employed to evaluate the impact of different qualities of water applications to almonds at different growth stages on the water balance and salinity dynamics in the soil.

The objectives of this study are (1) to calibrate and validate HYDRUS-2D to describe water content distributions and spatiotemporal salinity dynamics in the soils under sprinkler-irrigated almond with recycled water, (2) to simulate water movement and salinity dynamics for other experimental irrigation treatments including substituting less saline irrigation water for the resident recycled water irrigation at three phenologically different growth stages, and (3) to evaluate the water use efficiency of almonds under the different irrigation treatments.

2. Materials and methods

2.1. Experimental details

The experimental site was established at a mature almond plantation located in the Northern Adelaide Plains irrigation district, approximately 35 km north of Adelaide, South Australia (34.628°S and 138.683°E). The orchard was planted in 1998 and designed to have two adjacent rows of a commercial variety, Nonpareil, bordered on either side by pollinators, Price and Keane. All trees were grafted to Bright peach hybrid rootstock with rows planted in a north-south direction. Trees were spaced at a distance of 5.5 m within the rows and 7.5 m between rows.

The trial was designed as a randomized unblocked design, with four treatments replicated four times, plus an additional demonstration plot. Each treatment plot consisted of micro-sprinklers (five trees) along a tree line and was three rows wide. It covered a double row of Nonpareil trees plus a single row of a pollinator variety. All soil and plant measurements were collected from the three central trees in the middle row. The treatment infrastructure was installed before the 2013–14 irrigation season and was designed to substitute recycled (more saline) water irrigation (2 seasons average EC_{iw} = 1.9 dS/m) with less saline water (2 seasons average EC_{iw} = 0.78 dS/m) at one of the three phenological growth stages. The treatment when recycled water irrigation was used for the entire irrigation season represents the control treatment (A). In treatment B, less saline water was applied between the buds burst and pit hardening (BB-PH) stages. In treatment C, less saline irrigation was applied between the pit hardening and harvest (PH-H) stages, whereas in treatment D, less saline irrigation was applied between the harvest and leaf fall (H-LF) stages. The number of days during the three physiological stages when less saline water was applied in treatments B, C, and D was 84, 108, and 73 during 2014–15 and 88, 101, and 88 during and 2015–16, respectively. In addition, a non-replicated plot (treatment E) of trees was irrigated with less saline water during the entire season for demonstration purposes. Table 1 gives details about the four replicated irrigation treatments and the non-replicated demonstration treatment. Further details about the trial design are described in Pitt et al. (2015).

Irrigations were scheduled to replace estimated tree evapotranspiration, which was evaluated based upon a modified version of the protocol developed by the Almond Board of Australia (2011). The Almond Board of Australia (ABA) provides a spreadsheet based on a

Table 1
The timing of exposure to non-saline irrigation water in treatments A–D (replicated) and treatment E (a non-replicated demonstration plot).

Treatments	Irrigation	Growth Stages		
		1	2	3
		BB* to PH#P#	H to H^λ^	H to LD^η^
A - Control	Saline all year	Saline		
B	Non-saline at BB-PH	Non-saline	Saline	
C	Non-saline at PH-H	Saline	Non-saline	Saline
D	Non-saline at H-LD	Saline		Non-saline
E	Non-saline all year	Non-saline		

* Bud burst.
\# Pit hardening.
λ Harvest.
η Leaf drop.

water budgeting tool to facilitate this process. The spreadsheet requires the user to enter daily estimates of pan evaporation from a class A pan installed on their property and uses "in-house" crop factors (C_f) within the spreadsheet to calculate the crop water requirement for the day (Almond Board of Australia, 2011). The potential crop water use (ET_C) is the result of a product of measured pan evaporation (ET_{pan}) and a given crop factor on any particular day during the season. Therefore, data on irrigation depths for the experimental site were sourced from the collaborating grower and cross-checked against flow meters located in each treatment plot. Applied depths of irrigation were recorded weekly through the irrigation season to ensure the same depth of irrigation was applied to all treatments at each growth stage. The amount of seasonal irrigation to almonds was slightly higher (8%) during 2015–16 as compared to 2014–15. The orchard was irrigated with Ein-Dor (70 L/h) micro-sprinklers spaced every 5.5 m, halfway between trees, along the length of tree rows spaced at 7.5 m. This resulted in an application rate of 1.7 mm/h. The spatial extent of sprinklers was over a 280-cm radial area and there was a small overlap from neighboring sprinklers. Irrigation water was distributed more or less uniformly on the soil surface along a tree row to a distance of 280 cm on both sides of the tree line. While sprinkler irrigation with saline water can cause direct salt injury to the crop foliage, it remained an understory intervention for almond trees at the experimental site.

The recycled water was drawn from the Bolivar Wastewater Treatment Plant. The wastewater used for irrigation in this study was class A recycled water and as per the guidelines Class A water has received a level of treatment greater than classes B to D and is suitable for unrestricted irrigation to all crops and fodder types (Department of Human Services and South Australian Environmental Protection Agency, 1999). The less saline irrigation water was supplied with a potable water connection (SA Water), installed in 2013 adjacent to the trial site. Water samples were continuously collected throughout the growing season via sprinklers, and the electrical conductivity of the irrigation water (EC_{iw}) was assessed. In treatment A (recycled water), the EC_{iw} varied from 1.01 to 2.54 and 1.2–2.18 dS/m during 2014–15 and 2015–16 seasons, respectively, with corresponding average EC_{iw} of 1.94 dS/m and 1.81 dS/m. Similarly, in treatment E (less saline water), the EC_{iw} varied from 0.72 to 0.78 dS/m (average 0.76 dS/m) and 0.83–0.86 dS/m (average 0.85 dS/m), respectively during 2014–15 and 2015–16.

The experimental site was managed as per standard commercial orchard practices including a full nutrient, fungicide, and herbicide spray program plus mechanical harvest operations. A mid-row cover crop of various volunteer weeds and grasses (both annual and perennial) were controlled with occasional slashing and under tree herbicide operations. The experimental site was fertilized via foliar, broadcast and fertigation methods as reported in Pitt et al. (2015). The variation in EC_{iw} due to fertigation was not considered in the modeling simulations as the amount and timing of fertilization application is similar across all the treatments.

Soils at the site consist of a sandy loam to loam in the surface 35-cm horizon, followed by hard and calcareous clay (35–110 cm), and variable clay soil zoning below 110 cm, as characterized by Dowley and Fitzpatrick (2001). They noted that the tree root development is good in the upper 0.6 m of the profile and reported good water movement in the surface layer, with 24-h irrigation (at a rate of 2.5 mm/h) wetting the soil to a depth of 45–50 cm. The moisture characteristics, bulk density, soil textures, particle size distribution, and chemical properties of the soils of this region have also been documented in the APSIM Soil database (2016) and the ASRIS (2011) database. The particle size distribution and the bulk density of various depths were used to estimate the soil hydraulic parameters using ROSETTA (Schaap et al., 2001), a pedo-transfer function software package that uses neural networks to predict soil hydraulic parameters from soil texture and related data. However, values of residual (θr) and saturated (θs) water contents were taken from the databases mentioned above. The values of soil hydraulic parameters (α, n, and Ks) were further optimized during calibration. The optimized soil hydraulic parameters for different soil depths used in the present modeling study are given in Table 2.

Table 2
Optimized soil hydraulic parameters at the experimental site used in the HYDRUS-2D simulations.

	Soil depth (cm)	Texture	θ_r	θ_s	α	n	K_s	l
			$cm^3\ cm^{-3}$		cm^{-1}	–	cm/day	–
1	0–15	Sandy loam	0.06	0.42	0.075	1.89	120	0.5
2	15–25	Loam	0.12	0.37	0.059	1.48	80	0.5
3	25–35	Sandy clay loam	0.18	0.40	0.041	1.40	65	0.5
4	35–55	Clay loam	0.23	0.45	0.027	1.23	40	0.5
5	55–110	Clay loam	0.22	0.40	0.045	1.40	70	0.5
6	110–130	Silty clay loam	0.19	0.37	0.02	1.20	30	0.5
7	130–150	Silty clay loam	0.20	0.38	0.032	1.32	40	0.5
8	150–200	Silty clay loam	0.19	0.37	0.02	1.20	30	0.5

2.2. Meteorological data

HYDRUS-2D requires daily rainfall, potential evaporation (E_s), and transpiration (T_p) as inputs, which define the dynamic climatic variability experienced by a plant. Data on rainfall and daily reference evapotranspiration (ET_0) during the modeling period (2014–15 and 2015–16) for the experimental site were generated by running a data drill (Jeffrey et al., 2001) which generate the data for a site depending on the available climate data records in the adjoining Bureau of Meteorology (BOM) observatories. The observatories closest to the experimental site are Edinburg Raaf (6.9 km), Roseworthy (16 km), and Parafield (16 km). Crop coefficients (K_c), which were obtained from the IRES irrigation scheduling software developed by Rural Solutions SA (Rural Solutions SA, 2011), were used to estimate daily ET_C for almonds. Daily ET_C was divided into potential T_p and E_s following Belmans et al. (1983) using measured LAI at the experimental site. LAI was determined using the method described in Fuentes et al. (2014) using an SLR Camera (Leica Digilux 2, New Jersey, USA). LAI was measured three times during both seasons: just after pit-hardening (November), before harvest (February), and in the weeks approaching senescence (April). Four under canopy images were collected from each of three central trees using a sensor located at the ground level and 1.5 m away from the trunk. Four images captured the north, south, east, and west portions of the canopy. Images were processed using an algorithm developed by Fuentes et al. (2014). Daily potential T_p and E_s values were then used as time-variable atmospheric boundary conditions in the model, along with precipitation data for the site during the simulation period. Seasonal rainfall at the experimental site amounted to 327 and 373 mm during 2014–15 and 2015–16 seasons, respectively. Daily ET_0, rainfall, and the amount of irrigation applied to almonds during the 2014–15 and 2015–16 seasons are shown in Fig. 1.

2.3. Water content and soil salinity measurements

Soil water contents were measured on a monthly basis during the 2015 and 2016 irrigation seasons using a 503 DR Hydroprobe neutron moisture meter (CPN International, California, USA). Twelve aluminum access tubes were installed in May 2014 for the monitoring of spatio-temporal moisture contents distribution in the soil in different treatments. The tubes were installed in three replicates in treatments A, C, and D, two replicates in treatment B, and a single replicate in the non-replicated treatment E. Access tubes were installed 90 cm from the sprinkler emitters across the tree line. The probe was setup to measure at 10 cm depth increments between 20 and 60 cm and 20 cm depth increments between 60 and 200 cm. At the same time, undisturbed soil samples were collected from three separate cores for the determination

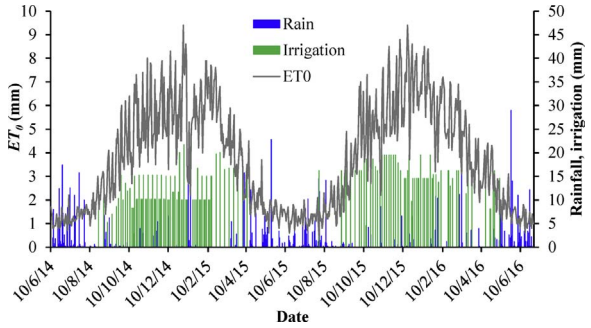

Fig. 1. Daily reference crop evapotranspiration (ET_0, line graph), rainfall (blue bars), and irrigation (green bars) applied to almonds during 2014–15 and 2015–16. (For interpretation of the references to colour in this figure legend, the reader is referred to the web version of this article.)

of bulk density, for the conversion of gravimetric to volumetric water contents, and for the calibration of the Neutron Probe.

Soil samples were collected from every plot of all treatments at the beginning of 2014–15 and at the end of each growth stage (bud burst, pit hardening, harvest) during the 2014–15 and 2015–16 seasons. Samples were collected 100 cm into the mid-row from the sprinkler emitter and in 10 cm increments to a depth of 160 cm using a hydraulic soil sampling rig with a 50 mm diameter collection tube (Christies Engineering, Horsley Park, Australia). Soil salinity was measured as the electrical conductivity of 1:5 soil:water extracts (EC1:5) on duplicate samples using a temperature compensated conductivity meter (model CON510, Eutech, Singapore). However, soil salinity was reported as the electrical conductivity of the extract from a saturated paste (EC_e) using a conversion factor ($EC_e = 5.89 \times EC_{1:5}$, $R^2 = 0.72$) that was generated by analyzing paired data from 35 soil samples covering all depths, which had been split so that both $EC_{1:5}$ and EC_e could be measured. All salinities were determined following the method of Rayment and Higginson (1992). More details about the sampling and the analysis are described in Pitt et al. (2017).

2.4. Root distribution

Most almond roots at the experimental site are distributed in shallow depths (0–25 cm). Very few roots were encountered in the 25–50 cm depth due to the presence of hard clay at the shallow depth, which doesn't allow the roots to penetrate deeper as the penetration resistance exceeds 2 MPa (Dowley and Fitzpatrick, 2001). The root distribution considered in the model was based on a rough estimate of the volume of roots recovered from various depth ranges (in increments of 10 cm from the surface to a depth of 160 cm) from soil samples collected using a hydraulic rig. As the roots were only observed above the 50 cm soil depth, their distribution was assumed in the model within the 0–50 cm region with a maximum root density at the 20-cm soil depth. Root water uptake from this region was computed using the Feddes macroscopic approach (Feddes et al., 1978) implemented in the HYDRUS software. The following critical values of pressure heads for almond in the Feddes et al. (1978) model were used: $h_1 = -10$, $h_2 = -25$, $h_3 = -500$ to -800, and $h_4 = -15000$ cm. These values were taken from previous investigations in South Australia (Phogat et al., 2012, 2013). The reduction of root water uptake due to salinity stress, $\alpha_2(h_\phi)$, was described by adopting the salinity threshold and slope function (Maas, 1990). The salinity threshold (EC_T) for almonds has a value of EC_e of 1.5 dS m^{-1} and a slope (s) of 19%. As required by HYDRUS-2D, these values were converted into the electrical conductivity at the actual soil water content (EC_{sw}), utilizing the linear relationship (Pitt et al., 2017) and initial water content values.

2.5. Soil salinity simulation

The distribution of soil solution salinity (EC_{sw}) was simulated as a non-reactive solute (Ramos et al., 2011; Phogat et al., 2012; Phogat et al., 2014; Wang et al., 2014). These studies demonstrated a good prediction of salinity under intensive irrigation and fertigation, similar to practices in the region under study. The longitudinal dispersivity was assumed as one/tenth of the modeling domain (with the transverse dispersivity being one-tenth of the longitudinal dispersivity) (Beven et al., 1993; Cote et al., 2003) and molecular diffusion in water equal to 1.66 cm^2/day (Phogat et al., 2014). Measured values of irrigation water salinity (EC_{iw}) were used as a time variable input for the root zone soil salinity prediction. The rainfall chemistry analyzed by Cresswell et al. (2010) for different locations in Australia provided reliable information about rainfall salinity (EC_{rw}) for the Adelaide region, which is close to the experimental site. The average salinity of rainfall was 0.12 dS/m, and this value was used for all salinity simulations.

2.6. Modeling domain and initial and boundary conditions

A two-dimensional modeling domain was constructed with a width equal to the half distance between tree lines (375 cm) and a vertical depth of 200 cm (Fig. 2). The domain represents a right half cross-section of the almond tree plant spacing. The domain was discretized into 23,505 elements, with a finer mesh size on the upper boundary where the time-variable flux and atmospheric boundary conditions were imposed. Measured values of water contents and soil salinities, recorded on 10/6/2014, were used as the initial conditions. The water contents were measured using a Neutron Probe, and soil salinity was measured on disturbed soil samples collected during the probe calibration. The top boundary consisted of a time-variable flux boundary condition along the 280-cm width and an atmospheric boundary condition on the rest of the upper boundary (100 cm). A 15% rainfall interception by the tree was assumed, which is comparable to the reported value for similar deciduous trees (Xiao et al., 2000). Uniform distributions of net rainfall and irrigation were imposed as a time-variable flux boundary condition. However, the understory rainfall distribution and interception by trees could vary depending on the

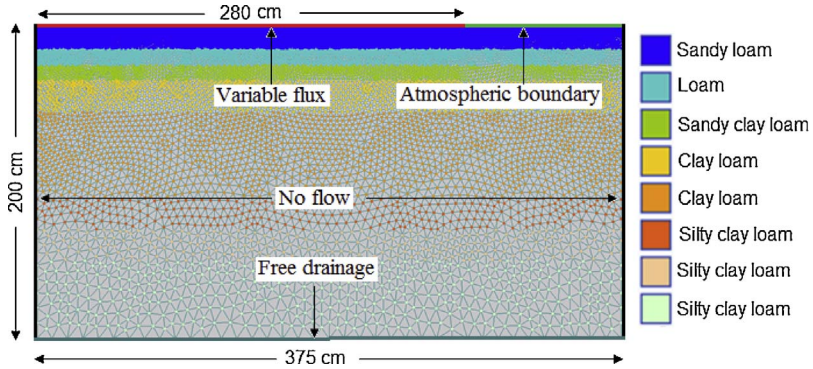

Fig. 2. A modeling domain (375 × 200 cm in the X–Z plane) representing the right half spacing of the mid-row along the almond tree line, showing imposed boundary conditions and the distribution of soil textural layers in the soil profile at the experimental site.

canopy characteristics. The side boundaries were no flow boundaries, and free drainage was imposed at the lower boundary. The model was calibrated using water content and salinity distributions during the entire season (July 10, 2014, to June 30, 2015). The model simulated soil solution salinity values (EC_{sw}) were converted to the soil salinity at saturation (EC_e) utilizing the corresponding water content data and a relation developed for the experimental soil samples. Validation was performed using data from July 1, 2015 to June 30, 2016 in the control (recycled water irrigation) (treatment A) by comparing measured and simulated values of the water contents and salinities at various depths (20, 30, 40, 50, 60, 80, 100, 120, 140, and 160 cm). In treatment A, irrigations were composed of recycled water having an average EC_{iw} of 1.94 dS/m (varied from 1.01 to 2.54 dS/m) and 1.81 dS/m (ranged from 1.2 to 2.18 dS/m) during the 2014–15 and 2015–16 seasons, respectively.

The calibrated and validated model was then used to simulate water and salinity dynamics under other treatments (B, C, and D) where recycled water was substituted with less saline water (EC_{iw} of < 0.8 dS/m) between different phenological stages of the almond growth. Simulations were also performed for treatment E where less saline water was used throughout the almond season. Simulated spatio-temporal dynamics of water contents and soil salinities were compared with the corresponding measured values in all treatments.

2.7. Yield components and water productivity

The yield was measured on the three central trees of each treatment plot. Prior to commercial harvest operations, the orchard floor was raked clear under the target trees. Trees were mechanically shaken on 16 February 2015 and 10 February 2016. Nuts were left to dry on the ground for four days before the experimental pickup operation.

Water productivity of almonds for actual ET losses ($WPET_C$) was estimated using the average seasonal ET_C values obtained from HYDRUS-2D simulations for two seasons and measured average yield data for different treatments given as:

$$WPET_C = \frac{Y}{ET_C} \tag{1}$$

where Y is the average kernel yield (kg/tree) and ET_C is the average seasonal actual evapotranspiration (m^3 of water/tree) estimated by HYDRUS-2D for different treatments.

2.8. Statistical parameters

The model's performance was evaluated by comparing measured (M) and HYDRUS-2D simulated (S) values of water contents and electrical conductivities (EC_e) in the soil at different times, and calculating the mean error (ME), the mean absolute error (MAE), and the root mean square error ($RMSE$) as follows:

$$ME = \frac{1}{N}\sum_{i=1}^{N}(M_i - S_i) \tag{2}$$

$$MAE = \frac{1}{N}\sum_{i=1}^{N}|M_i - S_i| \tag{3}$$

$$RMSE = \sqrt{\frac{1}{N}\sum_{i=1}^{N}(M_i - S_i)^2} \tag{4}$$

Model efficiency (E) was estimated as proposed by Nash and Sutcliffe (1970), which is given as:

$$E = 1 - \frac{\sum_{i=1}^{N}(M_i - S_i)^2}{\sum_{i=1}^{N}(M_i - \overline{M})^2} \tag{5}$$

The range of E lies between $-\infty$ and 1.0 (perfect fit). An efficiency value between 0 and 1 is generally viewed as an acceptable level of performance. Additionally, the coefficient of determination (R2) between the simulated and measured water contents and soil salinities was also estimated as:

$$R^2 = \left(\frac{\sum_{i=1}^{N}(M_i - \overline{M})(S_i - \overline{S})}{\sqrt{\sum_{i=1}^{N}(M_i - \overline{M})^2}\sqrt{\sum_{i=1}^{N}(S_i - \overline{S})^2}}\right)^2 \tag{6}$$

3. Results and discussion

3.1. Model calibration and validation for water content distributions in the soils

Model calibration and validation were performed using measured values of water contents in the soil at different depths and at different growth stages of almond in the saline water treatment (A; control). Measured and simulated water contents at different times during model calibration (2014–15) are compared in Fig. 3a–d. Different figures represent different growth stages of almond (bud burst, pit hardening, harvest, and leaf drop). The simulated distribution (S) of the water content in the soil profile matched well with the measured (M) values at all times during the growing season. However, there was a small over-estimation of water contents at the harvest stage (Fig. 3c) between the 60–120 cm soil depth. Such occasional deviations in simulated values are unavoidable and are on the same order of magnitude as measurement errors of the sensors (e.g., Ganjegunte et al., 2012; Evett et al., 2012).

Similarly, statistical errors (see Section 2.8) evaluating differences between measured and simulated soil water contents indicated a close fit (Table 3, the first row). The RMSE and MAE values obtained by comparing measured and simulated soil water contents at different depths and at different times varied from 0.020 to 0.036 and 0.014–0.030 $cm^3\,cm^{-3}$, respectively. Similarly, the mean error estimated at different times also varied in a narrow range (-0.030–$0.015\ cm^3\,cm^{-3}$) (Table 3). The negative ME values indicated a slight under-estimation of water contents by the model. However, small ME values indicate a good match between measured and simulated values. Also, the seasonal modeling efficiency of 0.79 indicates that the model provided a good representation of water movement under experimental conditions. Similarly, the coefficient of determination (R2; 0.85) for measured and simulated water contents also showed a close correspondence. Hence, estimated values of soil hydraulic parameters used in the model represent well the experimental soil.

During validation, the calibrated HYDRUS-2D model was run with the weather and irrigation input (treatment A) for the second season (2015–16). Overall, there was a good match between modeled and measured water contents at different depths and times as shown in Fig. 3e–h. Small deviations at some depths are common under field conditions. Similarly, the statistical comparison between measured and simulated soil water contents during validation (2015–16) showed a slightly wider error range (Table 3) as compared to calibration. However, the RMSE (0.16–0.38 cm^3cm^{-3}), MAE (0.11–0.34 $cm^3\,cm^{-3}$), and ME (-0.034–$0.006\ cm^3\,cm^{-3}$) values ranged within accepted limits reported in similar studies (e.g., Deb et al., 2011; Phogat et al., 2012, 2013, 2014, 2017; Ramos et al., 2011, 2012). The seasonal modeling

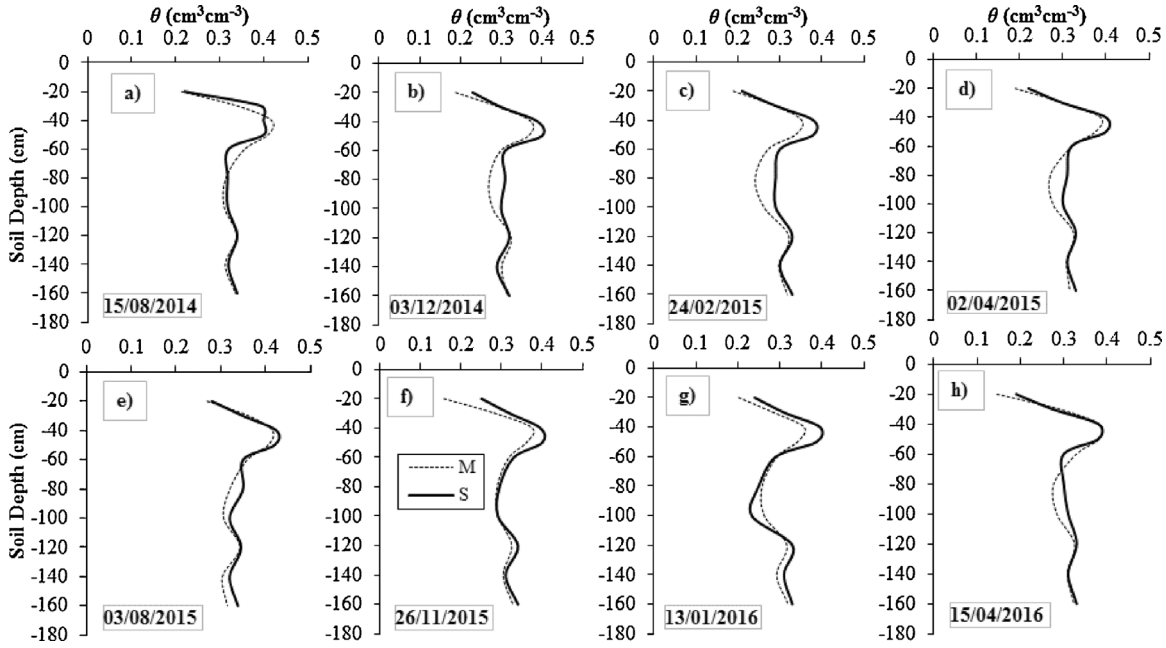

Fig. 3. Comparison of measured (M) and HYDRUS-2D simulated (S) water content distributions in the soil at indicated times during 2014–15 (a, b, c and d) and 2015–16 (e, f, g and h) under almond irrigated with saline water (treatment A).

efficiency (0.78) was also slightly lower than the corresponding value obtained during calibration. However, the R^2 value (0.86) between measured and simulated seasonal water content distributions indicated a close match. All statistical measures comparing measured and simulated water contents during calibration and validation thus indicate that HYDRUS-2D is able to reliably simulate water distribution patterns in the soil under evaluated experimental conditions during the entire almond growing season.

3.2. Water content distributions in other treatments

The calibrated and validated model was then used to simulate water content distributions in other treatments (B, C, D, and E) where irrigations with recycled water were substituted with less saline water during different growth stages. Water content distributions in these treatments (B, C, D, and E) during both seasons (2014–15 and 2015–16) at selected times are compared in Fig. 4. Water content depth distributions showed a good match between measured and simulated values at the bud burst growth stage in treatment B (see the second column in Fig. 4) and at the pit hardening stage in treatment C (see the third column in Fig. 4). However, there was a small over-estimation in water contents at the harvest stage in treatment D (see the fourth column in Fig. 4) at depths between 40 and 140 cm depth. Nevertheless, the statistical measures, such as error parameters (RMSE, MAE, and ME), model efficiency and R^2 between measured and simulated water contents, indicated a good match in all treatments (Table 3).

Despite some deviations, simulated results have shown a fairly good agreement with measured water contents in all treatments, as substantiated by different statistical error parameters, the model efficiency, and R^2 values. Similar deviations between measured and simulated water contents have been reported in other similar investigations (e.g., Ramos et al., 2012; Phogat et al., 2012, 2013, 2017; González et al., 2015). The extent of deviations can be attributed to various causes, possibly including different root distribution characteristics due to soil heterogeneity, which was assumed constant in all treatments. Modifying input parameters and calibrating the model for each treatment would probably improve HYDRUS-2D predictions for each treatment. Other causes for deviations between measured and simulated water contents, which could also be involved in the current investigation, were explained by Ramos et al. (2012) and are related to field measurements, model inputs, and model structural errors. Additionally, the measurement of soil water contents by sensors is also not free of errors,

Table 3
Statistical errors (RMSE, MAE, ME), model efficiency, and the coefficient of determination (R2) for the comparison between measured and simulated soil water contents for different treatments during 2014–15 and 2015–16.

Treatment	Year	RMSE	MAE	ME	Model efficiency	R^2
		($cm^3\ cm^{-3}$)				
A	2014–15[a]	0.020–0.036	0.014–0.030	−0.030 to 0.015	0.79	0.85
	2015–16[b]	0.016–0.038	0.011–0.034	−0.034 to 0.006	0.78	0.86
B	2014–15[b]	0.018–0.046	0.013–0.40	−0.040 to 0.026	0.72	0.73
	2015–16[b]	0.015–0.040	0.012–0.035	−0.032 to 0.010	0.74	0.80
C	2014–15[b]	0.015–0.62	0.011–0.058	−0.058 to 0.016	0.48	0.64
	2015–16[b]	0.017–0.60	0.014–0.056	−0.56 to −0.013	0.56	0.80
D	2014–15[b]	0.018–0.051	0.016–0.045	−0.038 to 0.020	0.46	0.57
	2015–16[b]	0.014–0.048	0.012–0.039	−0.034 to −0.002	0.60	0.74
E	2014–15[b]	0.017–0.040	0.015–0.036	−0.030 to 0.018	0.74	0.76
	2015–16[b]	0.025–0.048	0.022–0.037	−0.032 to 0.019	0.66	0.73

[a] Calibration period.
[b] Validation period.

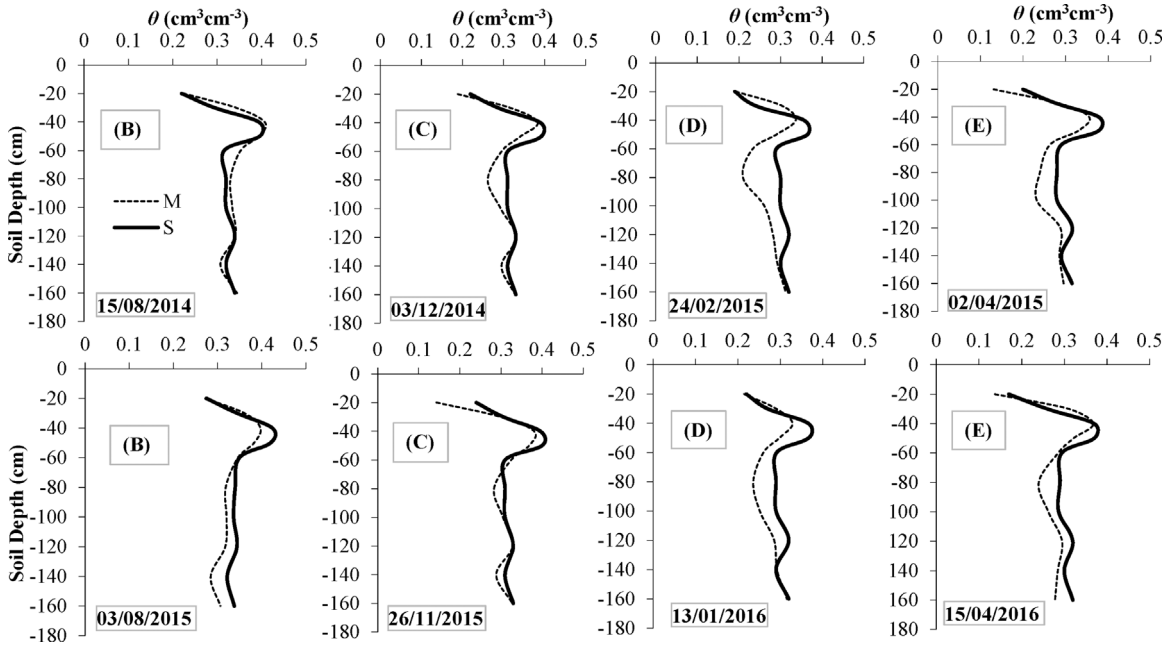

Fig. 4. Comparison of measured (M) and HYDRUS-2D simulated (S) water content distributions in the soil in different treatments (B, C, D, E) at indicated times during the 2014–15 (top row) and 2015–16 (bottom row) almond season.

due to numerous assumptions and inherent complexities in the soil (e.g., Rosenbaum et al., 2010; Ganjegunte et al., 2012; Evett et al., 2012), which may contribute to a similar extent of deviations in water contents as obtained by modelling predictions. Finally, the soil spatial variability in different treatments could lead to spatially dynamic root growth, which is not considered in the present modeling investigation.

3.3. Model calibration and validation for salinity dynamics in the soils

Simulated EC_e (S) dynamics in the soil profile under almond is compared with measured values at different times at 4 locations (A1, A2, A3 and A4) in treatment A during 2014–15 (Fig. 5a–d) and 2015–16 (Fig. 5e–h). During calibration (2014–15), there was a slight over-estimation of measured EC_e values at the bud burst stage between 40 and 80 cm soil depths. Thereafter, the model-produced EC_e dynamics remained within the extent of deviations observed in measured EC_e replicates at all stages of the almond growth. The statistical error parameters, i.e., RMSE, MAE, and ME estimated at different times between average measured and simulated EC_e values varied from 0.60 to 0.86, 0.47–0.56, and −0.35–0.49 dS/m (Table 4) and matched well with other studies (e.g., Ramos et al., 2012). The model efficiency (0.98) and R^2 (0.73) also indicated a close match between measured and simulated EC_e values during the entire season (2014–15).

Similarly, during the validation period (2015–16) simulated EC_e values at different depths and times are in close agreement with measured replicated values except for a small under-estimation in the

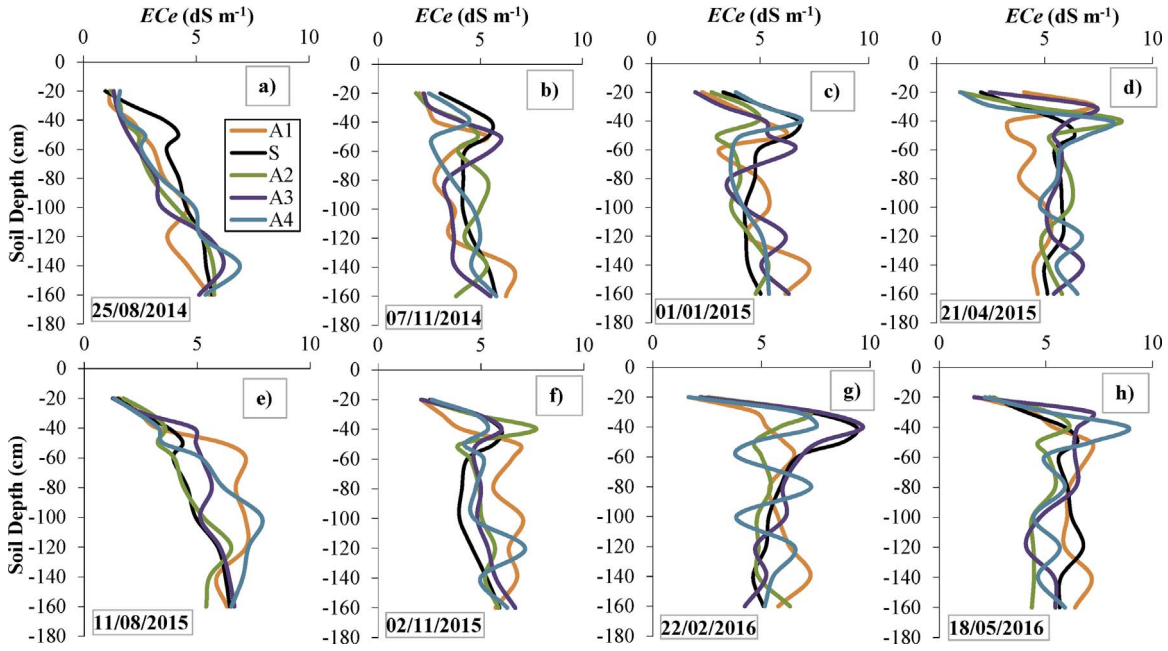

Fig. 5. Comparison of measured (at different locations A1, A2, A3 and A4) and HYDRUS-2D simulated (S) electrical conductivities in the soil at saturation (EC_e) at indicated times during 2014–15 (a, b, c, and d) and 2015–16 (e, f, g, and h) under almond irrigated with saline water (treatment A).

Table 4
Statistical errors (RMSE, MAE, ME), model efficiency, and the coefficient of determination (R2) for measured and simulated EC_e in the soil in different treatments during 2014–15 and 2015–16.

Treatment	Year	RMSE	MAE	ME	Model efficiency	R^2
		(dS m^{-1})				
A	2014–15[a]	0.60–0.86	0.47–0.56	−0.35 to 0.49	0.98	0.73
	2015–16[b]	0.71–1.09	0.57–0.90	−0.03 to 0.76	0.49	0.64
B	2014–15[b]	0.63–1.05	0.53–0.86	−0.66 to −0.29	0.44	0.69
	2015–16[b]	0.82–1.27	0.66–1.02	−0.55 to 0.62	0.32	0.51
C	2014–15[b]	0.59–0.85	0.44–0.69	−0.25 to 0.18	0.52	0.57
	2015–16[b]	0.64–1.20	0.46–0.82	−0.72 to 0.45	0.23	0.37
D	2014–15[b]	0.64–1.17	0.50–0.87	−0.67 to 0.12	0.43	0.54
	2015–16[b]	1.13–1.49	0.78–1.22	−1.09 to 0.69	0.20	0.37
E	2014–15[b]	0.83–1.26	0.72–1.06	−0.33 to 0.38	0.38	0.40
	2015–16[b]	0.50–1.60	0.49–1.32	−0.22 to 1.09	0.08	0.24

[a] Calibration period.
[b] Validation period.

60–140 cm soil depth at the pit hardening stage (Fig. 5e to h). The RMSE, MAE, and ME values between average measured and simulated EC_e values at different soil depths and growth stages varied from 0.71 to 1.09, 0.57–0.90, and −0.3–0.76 dS/m (Table 4). However, the model efficiency (0.49) and R^2 (0.64) values were lower compared to the corresponding valued observed during calibration (2014–15), which is a common occurrence.

3.4. Soil salinity dynamics in other treatments

The calibrated and validated model was then used to simulate salinity dynamics in the soil in other treatments (Fig. 6). Simulated salinity distributions in the soil in different treatments (B to E) were compared with corresponding measured EC_e replicates (B1, B2, and B3 for treatment B; C1, C2, C3, and C4 for treatment C; and D1, D2, D3, and D4 for treatment D) during both seasons. Simulated EC_e values remained within the measured range of different replicates during both seasons. However, small under- or over-estimations also occurred during some time in different treatments. Among the error estimates in treatment B, RMSE varied from 0.63-1.05 dS/m and MAE ranged from 0.53-0.86 dS/m during 2014–15 (Table 4). However, RMSE showed a wider range (0.82–1.27 dS/m) in the following season (2015–16). Similarly, MAE varied from 0.66-1.02 dS/m during 2015–16. Apart from these deviations, the model efficiency values (0.44 and 0.32) illustrate a reasonable prediction while R^2 values (0.69 and 0.51) indicate reduced congruency in the comparison. Overall, similar deviations in EC_e were recorded in treatment C (Table 4). However, deviations between measured and simulated EC_e in treatments D and E were comparatively larger as compared to other treatments (A, B, and C) but the variability remained within a reported range (Ramos et al., 2011, 2012).

Deviations between field-measured and simulated variables can be attributed to different causes, including errors related to field measurements, model inputs, and structural errors (Ramos et al., 2012). Ramos et al. (2012) have discussed extensively various causes that may result in deviations between field measurements and model simulations. In addition to various causes of errors mentioned in Ramos et al. (2012), an additional factor causing deviations in our study especially for EC_e values was the destructive sampling. While the model predicted the salinity dynamics at the same spot, field measurements were made at different locations each time. Moreover, the soils at the experimental site have immense spatial heterogeneity (nine different textures at different depths; Table 2), which had a strong impact on the measured

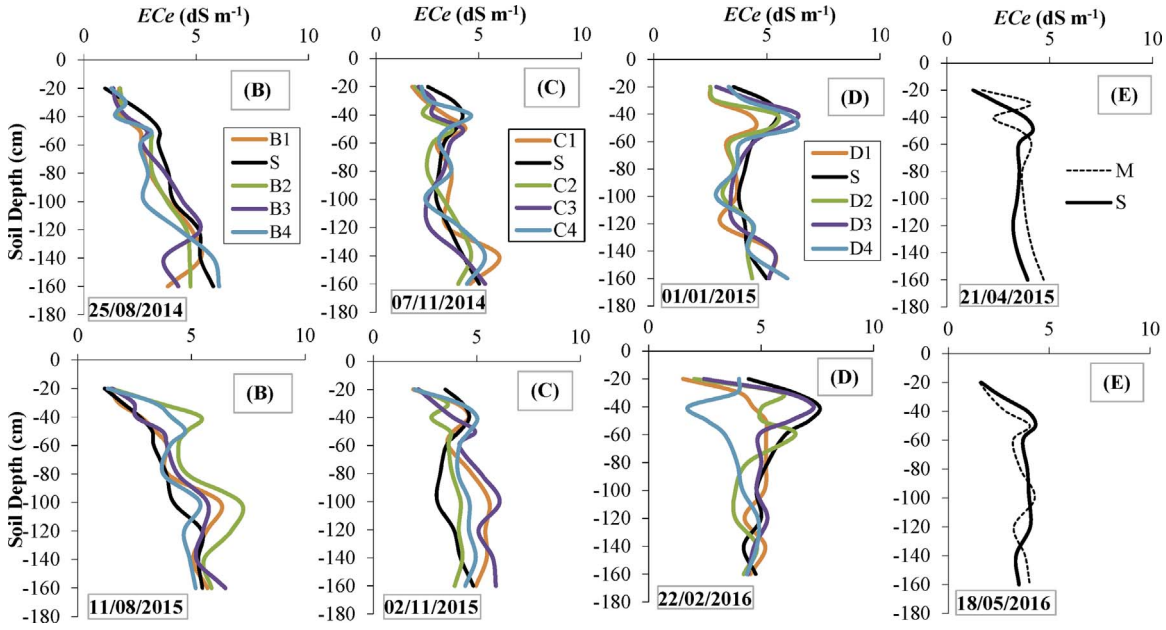

Fig. 6. Comparison of measured and HYDRUS-2D simulated (S) electrical conductivities in the soil at saturation (EC_e) in different treatments (B, C, D, E) at indicated times during the 2014–15 (top row) and 2015–16 (bottom row) almond seasons.

EC_e values as shown in different replicates in treatments A, B, C, and D. In treatment E, EC_e measurements were made only at one location and hence, there was a wider variation among measured and simulated EC_e values. The assumption of a similar conversion factor for EC_e and $EC_{1:5}$ for both years have also contributed to the extent of variability in estimated EC_e values.

The model input parameters, especially soil hydraulic parameters and solute dispersivities, may also introduce huge errors if not properly measured at the field site. In our study, these parameters were taken from other local studies or from the literature, which may have introduced errors in simulated values even though the model was properly calibrated and validated for the field site. Calibration and validation of the model only for one treatment could also result in errors in simulated values. In spite of these deviations between measured and simulated EC_e values, the error estimates are lower than reported in other studies (Ramos et al., 2011, 2012).

3.5. Seasonal water balance

The simulated water balance revealed that evapotranspiration losses (ET_C) by almonds under recycled water irrigations (treatment A) during 2014–15 amounted to 849.9 mm, which was 68.2% of the total applied water (rainfall + irrigation). Similarly, during 2015–16, although the seasonal ET_C (868.2 mm) was slightly higher, the drainage was reduced by 1% compared to the previous season. The error in the water balance simulations in A was 0.7 and 0.5% during 2014–15 and 2015–16 seasons, respectively, which is not uncommon in such situations. Deep drainage in treatment A represented 31.1% of the total applied water, which is an important amount of water that helps in transporting salts out of the root zone.

Monthly drainage fluxes below the 2-m soil depth under the almond tree irrigated with saline water (treatment A) during calibration (2014–15) and validation (2015–16) is shown in Fig. 7. Large deep drainage (80 mm) during July 2014 is the result of a low water requirement by the tree due to its dormancy and the early bud sprout stage coupled with high late winter rains. Deep drainage in other months during the first season (2014–15) varied between 13.7–39.2 mm. Deep drainage during September and October 2014 was very low because of a high water requirement by the almond tree during this period of profuse vegetative growth. Similarly, during 2015–16 more deep drainage (57.7 mm) occurred during the early season (August 2015) as compared to mid- and late-period. However, enormous deep drainage occurred during May and June months of the second season as compared to 2014–15. This was ascribed to higher rain during May-June 2016, which was almost double the amount

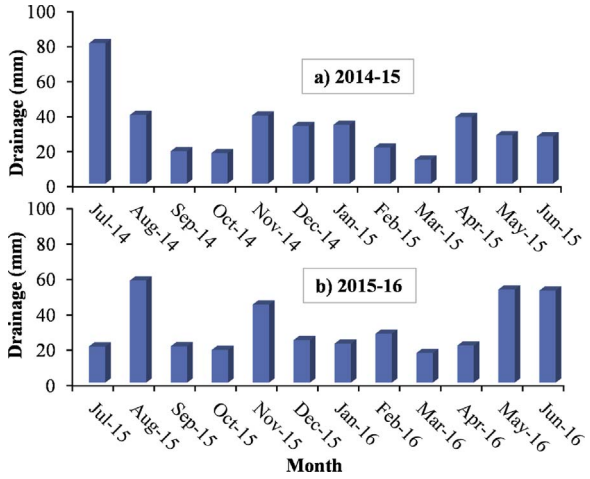

Fig. 7. Simulated monthly drainage (below the 2-m depth) under almond irrigated with saline water (treatment A) during (a) 2014–15 and (b) 2015–16.

Table 5
Seasonal water balance components for almond in different treatments (A, B, C, D, and E) during 2014–15 and 2015–16. Seasonal evapotranspiration, drainage and depletion/storage data was evolved from modelling simulations for different treatments. Water balance error represents the extent of error between source (irrigation, rainfall), sink (Evapotranspiration, drainage), and soil depletion/storage data. Depletion is considered as source term when final wetness in the soil was lower than the initial wetness and sink (storage) term if vice versa.

Treatments	Components	2014–15		2015–16	
		(mm)	(%)[#]	(mm)	(%)[#]
A	Irrigation	889.4	71.3	960.4	76.8
	Rainfall	326.9	26.2	372.7	29.8
	Soil depletion (+)/storage (−)	30.4	2.4	−81.8	−6.5
	Evapotranspiration (ET_C)	849.9	68.2	868.2	69.4
	Drainage	387.8	31.1	376.9	30.1
	Water balance error[*]	9	0.7	6.2	0.5
B	Irrigation	889.4	72.2	960.4	76.5
	Rainfall	326.9	26.5	372.7	29.7
	Soil depletion (+)/storage (−)	15.3	1.2	−78.2	−6.2
	Evapotranspiration (ET_C)	878.6	71.3	892.8	71.1
	Drainage	359.3	29.2	352.1	28.1
	Water balance error[*]	−6.3	−0.5	10	0.8
C	Irrigation	889.4	74.2	960.4	75.6
	Rainfall	326.9	27.3	372.7	29.3
	Soil depletion (+)/storage (−)	−18.29	−1.5	−62.1	−4.9
	Evapotranspiration (ET_C)	880.9	73.5	923.5	72.7
	Drainage	303.8	25.4	321.1	25.3
	Water balance error[*]	13.31	1.1	26.4	2.1
D	Irrigation	889.4	73.2	960.4	76.7
	Rainfall	326.9	26.9	372.7	29.8
	Soil depletion (+)/storage (−)	−2.1	−0.2	−80.9	−6.5
	Evapotranspiration (ET_C)	859.8	70.8	877.2	70.1
	Drainage	361.8	29.8	367.7	29.4
	Water balance error[*]	−7.4	−0.6	7.3	0.6
E	Irrigation	889.4	74.9	960.4	76.2
	Rainfall	326.9	27.5	372.7	29.6
	Soil depletion (+)/storage (−)	−28.1	−2.4	−72.6	−5.8
	Evapotranspiration (ET_C)	941.1	79.2	954.7	75.7
	Drainage	265.6	22.4	289.2	22.9
	Water balance error[*]	−18.5	−1.6	16.6	1.3

[*] is$(\sum source - \sum \sin k)$.
[#] represents% of source (irrigation + rainfall ± depletion/storage).

received during the same period of the 2014–15 season. This kind of rainfall during the dormant period could be helpful in driving salts out of the root zone. This suggests that the presence of higher amounts of salts in irrigation water not only reduced water uptake by almond trees but it may have also encouraged greater hydraulic flow through the soil profile. A similar monthly drainage pattern was observed in other treatment as well.

Simulated seasonal ET_C of almond in treatment B was increased by 3.4 and 2.8%, during 2014–15 and 2015–16, respectively, as compared to the corresponding values in treatment A (Table 5). This suggests that switching to irrigation with non-saline water during the bud burst and pit hardening stages exposed the almond tree to less osmotic pressure in the root zone and increased root water uptake, thereby increasing the water consumption. As a consequence, this favorable impact also reduced the drainage component by 6–7% compared to treatment A (Table 5). In treatment C, where less saline irrigation was used between the pit hardening and harvest stages, seasonal ET_C of almond increased as compared to the control treatment (treatment A). The extent of an increase in ET_C was also higher than in treatment B, especially during 2015–16. Seasonal ET_C increased by 3.6 and 6.4% during the 2014–15 and 2015–16 seasons, respectively, as compared to treatment A. On the other hand, seasonal drainage in treatment C was reduced by 21.7 and 14.8% during 2014–15 and 2015–16, respectively, as compared to treatment A, irrigated with saline water throughout the entire season. This suggests that the impact of switching to less saline irrigation on water uptake by almond was slightly more effective during the mid-stage of almond growth (treatment C) compared to the initial period

(treatment B). Similarly, seasonal ET_C of almond in treatment D was almost at par with that in treatment A, because it only increased by 1.2 and 1.0% during the 2014–15 and 2015–16 seasons, respectively, compared to treatment A (Table 5). Consequently, drainage losses also decreased by 6.7 and 2.4% during 2014–15 and 2015–16, respectively, as compared to the corresponding values in treatment A (recycled water irrigation). This shows that switching to less saline irrigation between the harvest and leaf fall stages had the least impact on water uptake by almond. During this period, the water demand is progressively reduced as the tree is dropping its leaves to enter into the dormant phase. Additionally, mechanical harvesting also influences water uptake as tree shaking causes considerable canopy defoliation and disturbs the natural soil-plant coherence.

Irrigation with less saline water during the entire season (treatment E) produced the highest amount of seasonal ET_C by almond (Table 5). Seasonal ET_C increased by 10.7 and 10% during the 2014–15 and 2015–16 seasons, respectively, as compared to irrigation with saline water (treatment A). This indicates early commencement of enhanced plant water use in non-saline treatment (Pitt et al., 2015). Moreover, the reduction in the osmotic stress due to fewer salts being added to the soil by irrigation (treatment E) played a key role in enhanced water uptake by the almond tree. Consequently, the lower osmotic pressures at the soil-root interface presumably resulted in a lower ionic stress within the leaf tissues, slowing the senescence of older leaves (Munns and Tester, 2008) and enhancing root water uptake. It is also well known that the almond tree is very sensitive to the soil salinity and a unit increase in EC_e in the root zone above threshold (1.5 dS/m) may reduce water uptake and hence almond yield by 19% (Maas, 1990). On the other hand, a decrease in drainage component amounted to 31.5 and 23.3% during 2014–15 and 2015–16, respectively, as compared to treatment A. This is quite significant and may have a great impact on salts leaching from the soil. Overall, the modeling error in the water balance ranged from −1.6 to 2.1% across all treatments, which indicates good simulations of the water balance under complex conditions.

3.6. Seasonal salinity dynamics

There is an increased chance of salts accumulation in the root zone in treatment A compared to the other treatments as the almonds were irrigated with recycled water with an average EC_{iw} of 1.94 dS/m (varied from 1.01- 2.54 dS/m) and 1.81 dS/m (ranges from 1.2- 2.18 dS/m) during the 2014–15 and 2015–16 seasons, respectively. During the first season, initial average root zone salinity (EC_e) drops steadily (Fig. 8) because of significant leaching as a result of high deep drainage during July 2014 (Fig. 8) generated by winter rain. A similar drop in the average root zone salinity also occurred during the 2015–16 season in all treatments. A notable difference between the two seasons was the lower initial average root zone salinity during the 2015–16 season in all the treatments. The root zone EC_e again increased during late September till mid-October in both seasons, which corresponds with a tremendous vegetative growth and an increased water requirement by the atmosphere, which may have reduced the leaching fraction and resulted in salts built up in the root zone. Another reason for an increase in EC_e in the soil during October was the high salinity of irrigation water as compared to the rest of the season. However, the average root zone EC_e in the soil during the mid-season fluctuated between 4 and 5 dS/m. On the other hand, the crop harvest and consequent leaf drop coupled with a reduced atmospheric demand and early winter rains had a tremendous impact on the sharp decline in the root zone EC_e during both seasons. Post-harvest irrigation also contributed to a gradual reduction in the EC_e due to an increased tendency of generating high deep drainage. Hence, the root zone salinity was reduced to a seasonal minimum level of 3.9 dS/m at the end of 2014–15. However, the minimum root zone EC_e of 3.7 dS/m in treatment A during the 2015–16 season was observed during September 2015 (Fig. 8), which was lower than the final EC_e (4.07 dS/m) in the soil.

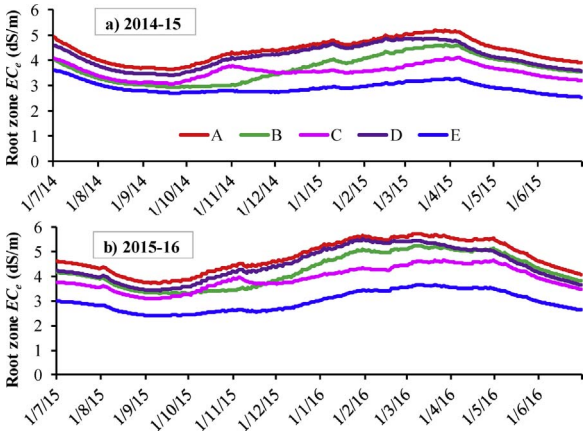

Fig. 8. Simulated average daily root zone EC_e in different treatments under almond during the (a) 2014–15 and (b) 2015–16 seasons.

Simulated daily average root zone salinity of the saturation extract (EC_e) in treatment B showed a similar seasonal pattern as observed in treatment A (Fig. 8). Nevertheless, the average EC_e was lower than in treatment A, especially between the bud burst to pit hardening stages when less saline water was applied in treatment B. Later on, although the salinity gradually increased, it remained below the corresponding EC_e in treatment A. In the following season (2015–16), a similar seasonal pattern was observed in daily EC_e in the root zone as observed during the previous year (2014–15).

In treatment C, the average root zone EC_e was slightly higher than the corresponding value in treatment B during the initial stage of 2014–15. However, the EC_e later on reduced in response to the application of less saline water between the pit hardening to harvest stages. Thereafter, the EC_e in treatment C remained lower than in treatment B until the end of the season. The average EC_e during 2015–16 also remained lower in treatment C as compared to treatment B since the same irrigation water was applied from the beginning to the end of the season except for a few days during the bud burst to pit hardening stages when less saline irrigation water was applied in treatment B. Hence, lower root zone salinity in treatment C than in treatment B supported higher seasonal water uptake reported in the previous section.

On the other hand, in treatment D during 2015–16, the daily salinity remained higher than in treatments B and C throughout the season, except in May-June when non-saline water was applied during the post-harvest stage. During the initial stage, the salinity was slightly lower than in treatment A. Thereafter, the average root zone EC_e in treatment D continued to remain close to that in treatment A during both seasons as irrigation was performed with recycled water with higher salts content. Hence, post-harvest irrigation with less saline water may prepare the soil for better root development in the ensuing season due to less osmotic stress. However, the impact is relatively short-lived as irrigation with saline water recommences at the beginning of the new season which increases the salt pressure again to the same level. Therefore, only a limited impact on root water uptake was observed when less saline water was applied during the harvest to leaf drop stages (D).

The average daily root zone EC_e in treatment E was much lower than in the other treatments during both seasons (2014–15 and 2015–16) as a result of the application of less saline water during the entire almond season (Fig. 8). However, the average EC_e remained higher than the almond threshold salinity (1.5 dS/m). This suggests that less saline water (EC_{iw} < 0.8 dS/m) adds enough salts into the soil that continue to build up during the season if they are not leached out of the root zone by applying more irrigation water. The comparison of season patterns of EC_e during the 2014–15 and 2015–16 seasons showed that the gap between treatment E and other treatments is widening throughout the

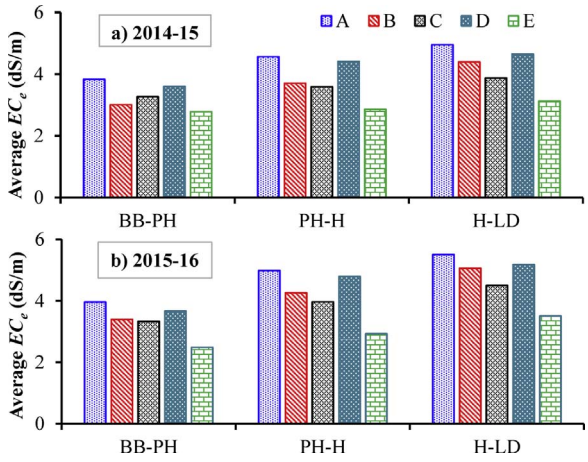

Fig. 9. Simulated daily root zone salinity (EC_e) in different treatments (A, B, C, D, and E) averaged for different growth stages (BB - Bud Burst, pH - Pit Hardening, H - Harvest, and LD - Leaf Drop) of almond during 2014–15 and 2015–16.

season over the years. Hence, these simulations need to be conducted for a longer time to fully understand the salinity dynamics over multiple years. This could have drastic implications on the judicious use of saline water for almond cultivation.

The model-simulated, daily root zone salinity averaged during different stages of almond growth in all treatments is shown in Fig. 9. It can be seen that the average salinity in treatment A remained higher than in other treatments as a result of the application of saline water irrigation during the entire almond growing season. The average EC_e was 3.8, 4.6, and 4.9 dS/m between the bud burst (BB)-pit hardening (pH), pH -harvest (H), and H-leaf drop (LD) growth stages, respectively, during 2014–15, while the corresponding EC_e during 2015–16 slightly increased to 4.0, 5.0 and 5.5 dS/m, respectively, during the same stages of almond growth. In contrast, the average EC_e was always lower in treatment E during all growth stages as compared to the other treatments since irrigation with non-saline water was applied during the entire season. Hence, the average EC_e of the root zone during the BB-pH, pH -H, and H-LD stages was 2.8, 2.9, and 3.1 dS/m, respectively, during 2014–15. While the salinity in treatment E during the following season (2015–16) decreased slightly during the BB-pH stage, it increased to 3.5 dS/m during the H-LD stage (Fig. 9). Overall, the average salinity in treatment E between the BB-pH, pH -H, and H-LD stages during 2014–15 decreased by 27, 37, and 37%, respectively, as compared to treatment A. However, the corresponding reduction during 2015–16 was 37, 41, and 36%, respectively. The seasonal average root zone EC_e over the two seasons in treatment E was reduced by 35% as compared to the corresponding EC_e in treatment A.

In the other treatments (B, C, and D), the average EC_e between different growth stages remained between values observed in treatments A and E (Fig. 9). However, the impact of switching to irrigation with less saline water during different growth stages in different treatments is worth noticing. For example, the average EC_e in treatment B during 2014–15 was lower than in treatments C and D between the BB-pH stages, which corresponds to the time when irrigation with less saline water was applied. However, this trend was not maintained in the following year (2015–16) where EC_e in treatment C was slightly lower than in treatment B. It must be noted that the average EC_e in treatment C was lower than in treatments B and D at all other growth stages. However, at the end of the seasons the average EC_e in treatment C was almost in the middle of values obtained in treatments A and E. Therefore, the average EC_e between the BB-pH, pH -H, and H-LD stages in treatment C was reduced by 15, 21, and 20%, respectively, as compared to those in treatment A. The seasonal average of the root zone EC_e over the two seasons was reduced by 13, 18, and 6.4% in treatments B, C, and D, respectively, as compared to treatment A. These results

Table 6
Yield (kernel in shell), simulated evapotranspiration (ET_C), and water use efficiency (WUE) by an almond tree in different treatments during the 2014–15 and 2015–16 seasons.

Treatments	Yield (kg/tree)	ET_C (m^3/tree)	WUE_{ETc} (kg/m^3)
2014–15			
A	8.57	35.06	0.24
B	8.59	36.24	0.24
C	8.92	36.34	0.25
D	8.55	35.47	0.24
E	9.25	38.82	0.24
LSD* (A–D)	NS		
2015–16			
	8.37	35.81	0.23
	8.44	36.83	0.23
	8.43	38.09	0.22
	8.57	36.18	0.24
	8.56	41.44	0.21
LSD* (A–D)	NS		

* Least Square Difference (LSD) for treatments A to D only. Treatment E had a single replicate, hence not included in the statistical analysis.

suggest that switching to irrigation with less saline water between the pH -H stages could produce a better outcome in terms of lower salinity in the root zone accompanied by increased root water uptake in this treatment. However, there could be different seasonal EC_e developments if similar amounts of less saline water were applied in all treatments. It must be noted that the volume of good quality water applied in treatment C was higher than volumes applied in treatments B and D.

3.7. Yield and water use efficiency of almonds

Yield attributes did not elicit a significant yield response to the timing of the reduced salt pressure (Table 6). Previous almond studies have suggested that yield components can be relatively insensitive to a stress in the first years of exposure and that residual effects tend to present in the subsequent years (Goldhamer and Smith, 1995). Similar investigations assessing the timing of salt stress on Colombard grapes also found a negligible yield response early in the life of the trial but that differences increased with time (Stevens et al., 1999). If yields within the current trial are to respond to salinity treatments, it is likely that changes will occur only once treatment carryover effects from preceding years are included. However, Sanden et al. (2014) concluded that almonds are capable of much higher yields under even more saline conditions than old published standards. The almond water use efficiency in relation to crop evapotranspiration (WUE_{ETc}; 0.24–0.25 kg m^{-3}) also did not show any treatment effect because there were non-significant differences in the yield and seasonal ET_C losses were also varied in a narrow range across all treatments. However, similar WUE values (0.20–0.33 kg m^{-3}) have been reported in several studies (Romero et al., 2004; Goldhamer et al., 2006; Girona et al., 2005; Egea et al., 2010; Goldhamer and Fereres, 2017). On the other hand, the WUE of almonds in the Riverland region of Australia (Phogat et al., 2013) was almost double (0.43 kg m^{-3}) the value estimated in this study (0.24–0.25 kg m^{-3}). Apart from high soil salinity, sub-soil constraints, saline water irrigation at the experimental site, growing conditions (solar radiation, warm temperatures) coupled with pests and diseases infestation, the density of plantings, the frequency of irrigation and fertigation played a key role in the wide disparity in the WUE_{ETc} at two locations. Although almonds are among the species capable of maintaining high gains in water productivity under increasing soil water deficit (Prichard et al., 1992; Goldhamer and Viveros, 2000; Girona et al., 2005; Phogat et al., 2013), a similar resilience under the osmotic stress has not yet been established. This behavior is due in part to the adaptation of trees to conditions with strong water stress by developing more compact crowns with a higher fruit density than those of fully irrigated trees (Egea et al., 2010). On the other hand, the

evaluation of the impact of timing of salinity stress (treatment effect) is more complex to ascertain as salts are highly dynamic in the soil system.

The average dry weight of a single kernel (1.08 g) and WUE_{ETc} of 0.25 kg m^{-3} suggest that 4 Liters of water are required to produce a single kernel, which is comparable to "one US gallon per nut" reported by Goldhamer and Fereres (2017). In fact, four liters of water account only for the pure form of water consumed by the tree to produce a single nut, neglecting the issues associated with all soluble salts remaining in the soil system. These salts may stockpile in the soil over years and can hamper the sustainable almond production if they are not removed from the root zone. On the other hand, high amounts of salts leached below the root zone can adversely affect groundwater resources and can inflict significant environmental damage. Hence, there exists a trade-off between irrigation with saline water and pollution hazards of groundwater resources, which requires special attention to sustainable water management practices. Such a production system has to deal with a "salinity paradox," which resembles the so-called "efficiency paradox" (Scott et al., 2014), a phenomenon that essentially overturns whatever is gained through improved water use efficiency (Ward and Pulido-Velazquez, 2008).

4. Conclusions

A numerical model (HYDRUS-2D) was successfully calibrated (2014–15) and validated (2015–16) using seasonal water content distributions and salinity dynamics in the soil under almond irrigated with different quality waters. Simulated results revealed that irrigation with saline water had a notable impact on the root zone salinity dynamics and almond water uptake. Seasonal evapotranspiration (ET_C) of almond decreased by 10% and the overall seasonal average root zone EC_e increased by 54% for trees receiving saline irrigation (two seasons average EC_{iw} of 1.85 dS/m) across the entire irrigation season as compared to trees receiving non-saline irrigation ($EC_{iw} < 0.8$ dS/m). Other treatments tested the response of trees to substituting saline water with non-saline water during three phenologically different growth stages: before pit-hardening, between pit-hardening and harvest, and following harvest. Despite the inter-treatment differences in timing and depth of saline and non-saline irrigation, the seasonal patterns of soil salinity (EC_e) were similar across all treatments. However, irrigation with non-saline water between different growth stages reduced the buildup of salts in the soil profile. Despite this reduction, the average root zone EC_e remained above the level of the almond salinity tolerance ($EC_e = 1.5$ dS/m) during the entire season even for soils that received less saline water during the entire irrigation season. The model suggested that winter rainfall was not very effective in reducing potentially high soil salinity levels below those that would not adversely influence the normal growth of the almond. Similarly, replacing irrigation with saline recycled water with non-saline water was ineffective in containing the root zone EC_e below the crop threshold. However, the substitution of less saline water during different growth stages resulted in insignificant differences in the yield. This suggests that the current salinity threshold (1.5 dS/m) for almond may need a comprehensive examination in light of this and other recent studies (e.g., Sanden et al., 2014). The results of this study also demonstrated that deep drainage below the root zone (2 m) is irregular, and its magnitude was highly varied during the almond season. This warrants further investigation, as does the development of appropriate reclamation strategies. Restricted drainage conditions, coupled with salts resurgence due to capillary action, may complicate adequate salt removal from the soil system.

Acknowledgements

The authors wish to thank the Australian Water Recycling Centre of Excellence, the South Australian River Murray Sustainability Program (SARMS 3IP) and the Goyder Institute for Water for funding this research. The leaves granted to Dr. Vinod Phogat by CCS Haryana Agricultural University for availing Post-Doctoral studies are highly acknowledged.

References

Šimůnek, J., van Genuchten, M.Th., Šejna, M., 2016. Recent developments and applications of the HYDRUS computer software packages. Vadose Zone J. 15 (7), 25. http://dx.doi.org/10.2136/vzj2016.04.0033.
ABA, 2011. Final Report. HAL Project 07005 – Sustainable Optimisation of Australian Almond Production. Technical Report. Almond Board of Australia. http://australianalmonds.com.au/documents/Industry/Fact%20Sheets/Crop%20water%20use%20Fact%20Sheet.pdf.
APSIM, 2016. Soil Database. https://www.apsim.info/Products/APSoil.aspx.
ASRIS, 2011. Australian Soil Resource Information System. (Accessed on July 20, 2017). http://www.asris.csiro.au.
Alcon, F., Egea, G., Nortes, P.A., 2013. Financial feasibility of implementing regulated and sustained deficit irrigation in almond orchards. Irrig. Sci. 31, 931–941.
Assouline, S., Russo, D., Silber, A., Or, D., 2015. Balancing water scarcity and quality for sustainable irrigated agriculture. Water Resour. Res. 51, 3419–3436. http://dx.doi.org/10.1002/2015WR017071.
Austin, J., Zhang, L., Jones, R.N., Durack, P., Dawes, W., Hairsine, P., 2010. Climate change impact on water and salt balances: an assessment of the impact of climate change on catchment salt and water balances in the Murray-Darling Basin, Australia. Clim. Change 100, 607–631.
Bahrami, V., Imani, A., Piri, S., 2015. Evaluation of almond cultivars growth characteristics under salinity stress. J. Noval Appl. Sci. 4 (12), 1227–1229.
Belmans, C., Wesseling, J.G., Feddes, R.A., 1983. Simulation of the water balance of cropped soil: SWATRE. J. Hydrol. 63, 271–286.
Ben-Asher, J., 1979. Errors in determination of the water content of a trickle irrigated soil volume. Soil Sci. Soc. Am. J. 43, 665–668.
Beven, K.J., Henderson, D., Reeves, A.D., 1993. Dispersion parameters for undisturbed partially saturated soil. J. Hydrol. 143, 19–43.
Bresler, E., McNeal, B.L., Carter, D.L., 1982. Saline and Sodic Soils: Principles-Dynamics-Modeling. Springer, Berlin, pp. 227.
Camposeo, S., Palasciano, M., Vivaldi, G.A., Godini, A., 2011. Effect of increasing climatic water deficit on some leaf and stomatal parameters of wild and cultivated almonds under Mediterranean conditions. Sci. Hort. 127, 234–241.
Cote, C.M., Bristow, K.L., Charlesworth, P.B., Cook, F.J., Thorburn, P.J., 2003. Analysis of soil wetting and solute transport in subsurface trickle irrigation. Irrig. Sci. 22, 143–156.
Cresswell, R.G., Dighton, J., Leaney, F., Vleeshouwer, J., Morrow, D., Harris, M., Stenson, M., 2010. Australia-wide Network to Measure Rainfall Chemistry and Isotopic Composition −Final Report of Project MD311, CSIRO, Water for a Healthy Country National Research Flagship, Australia.
Deb, S.K., Shukla, M.K., Mexal, J.G., 2011. Numerical modeling of water fluxes in the root zone of a mature Pecan orchard. Soil Sci. Soc. Am. J. 75, 1667–1680.
Dowley, A., Fitzpatrick, R., 2001. Almond production on the northern Adelaide plains: understanding your soil and water resource. Personal Commun (unpublished).
Egea, G., Nortes, P.A., Gonzalez-Real, M.M., Baille, A., Domingo, R., 2010. Agronomic response and water productivity of almond trees under contrasted deficit irrigation regimes. Agric. Water Manage. 97, 171–181.
Egea, G., Nortes, P.A., Domingo, R., Baille, A., Perez-Pastor, A., Gonzalez-Real, M.M., 2012. Almond agronomic response to long-term deficit irrigation applied since orchard establishment. Irrig. Sci. 31, 445–454.
Espadafor, M., Orgaz, F., Testi, L., Lorite, I.J., Villalobos, F.J., 2015. Transpiration of young almond trees in relation to intercepted radiation. Irrig. Sci. 33 (2015), 265–275.
Evett, S.R., Schwartz, R.C., Casanova, J.J., Heng, L.K., 2012. Soil water sensing for water balance, ET and WUE. Agric. Water Manage. 104, 1–9.
Feddes, R.A., Kowalik, P.J., Zaradny, H., 1978. Simulation of Field Water Use and Crop Yield. Simulation Monographs, Pudoc, Wageningen, The Netherlands.
Franco, J.A., Abrisqueta, J.M., Hernansáez, A., Moreno, F., 2000. Water balance in a young almond orchard under drip irrigation with water of low quality. Agric. Water Manage. 43, 75–98.
Ganjegunte, G.K., Sheng, Z., Clark, J.A., 2012. Evaluating the accuracy of soil water sensors for irrigation scheduling to conserve freshwater. Appl. Water Sci. 2, 119–125.
García-Tejero, I.F., Durán-Zuazo, V.H., Vélez, L.M., Hernández, A., Salguero, A., Muriel-Fernández, J.L., 2011. Improving almond productivity under deficit irrigation in semiarid zones. Open Agric. J. 5, 56–62.
García-Tejero, I.F., Hernández, A., Rodríguez, V.M., Ponce, J.R., Ramos, V., Muriel, J.L., Durán-Zuazo, V.H., 2015. Estimating almond crop coefficients and physiological response to water stress in semiarid environments (SW Spain). J. Agr. Sci. Tech. 17, 1255–1266.
Girona, J., Mata, M., Marsal, J., 2005. Regulated deficit irrigation during the kernel-filling period and optimal irrigation rates in almond. Agric. Water Manage. 75, 152–167.
Goldhamer, D.A., Fereres, E., 2017. Establishing an almond water production function for California using long-term yield response to variable irrigation. Irrig. Sci. 35, 169–179.
Goldhamer, D.A., Smith, T.E., 1995. Single-season drought irrigation strategies influence almond production. California Agric. 49, 19–22.
Goldhamer, D.A., Viveros, M., 2000. Effects of pre-harvest irrigation cut-off durations and post-harvest water deprivation on almond tree performance. Irrig. Sci. 19, 125–131.
Goldhamer, D.A., Viveros, M., Salinas, M., 2006. Regulated deficit irrigation in almonds:

effects of variations in applied water and stress timing on yield and yield components. Irrig. Sci. 24, 101–114.
González, M.G., Ramos, T.B., Carlesso, R., Paredes, P., Petry, M.T., Martins, J.D., Aires, N.P., Pereira, L.S., 2015. Modelling soil water dynamics of full and deficit drip irrigated maize cultivated under a rain shelter. Biosyst. Eng. 132, 1–18.
Gradziel, T.M., Kester, D.E., 1998. Breeding for self-fertility in California almond cultivars. Acta Hort. 470, 109–117.
Hassan, G., Persaud, N., Reneau, R.B., 2005. Utility of HYDRUS-2D in modeling profile soil moisture and salinity dynamics under saline water irrigation of soybean. Soil Sci. 170, 28–37.
Hassanli, M., Ebrahimian, H., Mohammadi, E., Rahimi, A., Shokouhi, A., 2016. Simulating maize yields when irrigating with saline water, using the Aqua Crop, SALTMED, and SWAP models. Agric. Water Manage. 176, 91–99.
Jeffrey, S.J., Carter, J.O., Moodie, K.B., Beswick, A.R., 2001. Using spatial interpolation to construct a comprehensive archive of Australian climate data. Environ. Modell. Softw. 16, 309–330.
Kandelous, M.M., Šimůnek, J., 2010. Numerical simulations of water movement in a subsurface drip irrigation system under field and laboratory conditions using HYDRUS-2D. Agric. Water Manage. 97, 1070–1076.
Maas, E.V., 1990. Crop salt tolerance. In: In: Tanji, K.K. (Ed.), Agricultural Salinity Assessment and Management 71. pp. 262–304 (Am. Soc. Civ. Eng., Reston).
Monks, D.P., Taylor, C., Sommer, K., Treeby, M.T., 2017. Deficit irrigation of almond trees did not decrease yield. Acta Hort. (ISHS) 1150, 251–260.
Munns, R., Tester, M., 2008. Mechanisms of salinity tolerance. Ann. Rev. Plant Biol. 59, 651–681.
Nash, J.E., Sutcliffe, J.V., 1970. River flow forecasting through conceptual models part I − A discussion of principles. J. Hydrol. 10, 282–290.
Nightingale, H.I., Hoffman, G.J., Rolston, D.E., Biggar, J.W., 1991. Trickle irrigation rates and soil salinity distribution in an almond orchards. Agric. Water Manage. 19, 271–283.
Nortes, P.A., González-Real, M.M., Egea, G., Baille, A., 2009. Seasonal effects of deficit irrigation on leaf photosynthetic traits of fruiting and non-fruiting shoots in almond trees. Tree Physiol. 29, 375–388.
Phogat, V., Mahadevan, M., Skewes, M., Cox, J.W., 2012. Modeling soil water and salt dynamics under pulsed and continuous surface drip irrigation of almond and implications of system design. Irrig. Sci. 30 (4), 315–333.
Phogat, V., Skewes, M.A., Mahadevan, M., Cox, J.W., 2013. Evaluation of soil plant system response to pulsed drip irrigation of an almond tree under sustained stress conditions. Agric. Water Manage. 118, 1–11.
Phogat, V., Skewes, M., Cox, J.W., Sanderson, G., Alam, J., Šimůnek, J., 2014. Seasonal simulation of water, salinity, chloride and nitrate dynamics under drip irrigated mandarin (*Citrus reticulata*) and assessing management options for drainage and nitrate leaching. J. Hydrol. 513, 504–516.
Phogat, V., Skewes, M.A., McCarthy, M.G., Cox, J.W., Šimůnek, J., Petrie, P.R., 2017. Evaluation of crop coefficients, water productivity, and water balance components for wine grapes irrigated at different deficit levels by a sub-surface drip. Agric. Water Manage. 180 (Part A), 22–34.
Pitman, M.G., Laüchli, A., 2002. Global impact of salinity and agricultural ecosystems. In: Laüchli, A., Lüttge, U. (Eds.), Salinity: Environment—Plants—Molecules. Kluwer Acad., Netherlands, pp. 3–20.
Pitt, T., Cox, J., Phogat, V., Fleming, N., Grant, C., 2015. Methods to Increase the Use of Recycled Wastewater in Irrigation by Overcoming the Constraint of Soil Salinity. Australian Water Recycling Centre of Excellence, Brisbane Australia.
Pitt, T., Phogat, V., Fleming, N., Cox, J., 2017. Almond Salt Sensitivity: Avoiding Salt Stress During Critical Growth Stages. Final Report of Project SARMS IRSPR1-010. South Australian Research and Development Institute, The State of South Australia.
Prichard, T.L., Asai, W., Verdegaal, P., Micke, W., Fuson, K., 1992. Effects of water supply and irrigation strategies on almonds. In: Proceedings of 20th Annual Almond Research Conference. Sacramento, USA. pp. 60–63.
Puerto, P., Domingo, R., Torres, R., Pérez-Pastor, M., 2013. Remote management of deficit irrigation in almond trees based on maximum daily trunk shrinkage. Water relations and yield. Agric. Water Manage. 126, 33–45.
Rajabpoor, S., Kiani, S., Sorkheh, K., Tavakoli, F., 2014. Changes induced by osmotic stress in the morphology, biochemistry, physiology, anatomy and stomatal parameters of almond species (*Prunus* L. spp.) grown *in vitro*. J. Forest. Res. 25 (3), 523–534.
Ramos, T.B., Šimůnek, J., Goncalves, M.C., Martins, J.C., Prazeres, A., Castanheira, N.L., Pereira, L.S., 2011. Field evaluation of a multicomponent solute transport model in soils irrigated with saline waters. J. Hydrol. 407, 129–144.
Ramos, T.B., Šimůnek, J., Goncalves, M.C., Martins, J.C., Prazeres, A., Pereira, L.S., 2012. Two-dimensional modeling of water and nitrogen fate from sweet sorghum irrigated with fresh and blended saline waters. Agric. Water Manage. 111, 87–104.
Rayment, G.E., Higginson, F.R., 1992. Saturation extracts. In: Rayment, G.E., Higginson, F.R. (Eds.), Australian Handbook of Soil and Water Chemical Methods. Inkata Press, Melbourne.
Romero, P., Botia, P., Garcia, F., 2004. Effects of regulated deficit irrigation under subsurface drip irrigation conditions on water relations of mature almond trees. Plant Soil 260, 155–168.
Rosenbaum, U., Huisman, J.A., Vereecken, H., Bogena, H.R., 2010. Sensor-to-sensor variability of the ECH2O EC-5, TE, and 5TE sensors in dielectric liquids. Vadose Zone J. 9, 181–186.
Rouhi, V., Samson, R., Lemeur, R., van Damme, P., 2007. Photosynthetic gas exchange characteristics in three different almond species during drought stress and subsequent recovery. Environ. Exp. Bot. 59, 117–129.
Rural Solutions SA, 2011. Irrigation and Crop Management Service, IRES Software, Version 4.0. Loxton Research Centre, Loxton, SA, Australia.
Sanden, B.L., Muhammad, S., Brown, P.H., Shackel, K.A., Snyder, R.L., 2014. Correlation of individual tree nut yield, evapotranspiration, tree stem water potential, total soil salinity and chloride in a high production almond orchard. In: Proc. ASABE Annual International Meeting Montreal. Quebec Canada July 13–16, Amer. Soc. Agric. and Bio. Eng.. (pp. 8).
Schaap, M.G., Leij, F.J., van Genuchten, M. Th., 2001. ROSETTA: a computer program for estimating soil hydraulic parameters with hierarchical pedotransfer functions. J. Hydrol. 251, 163–176.
Scott, C.A., Vicuña, S., Blanco-Gutiérrez, I., Meza, F., Varela-Ortega, C., 2014. 794 Irrigation efficiency and water-policy implications for river basin resilience. Hydrol. Earth Syst. Sci. 18 (4), 1339–1348.
Sorkheh, K., Shiran, B., Rouhi, V., Khodambashi, M., Sofo, A., 2012. Salt stress induction of some key antioxidant enzymes and metabolites in eight Iranian wild almond species. Acta Physiol. Plant 34, 203–213.
Stevens, R.M., Harvey, G., Partington, D.L., Coombe, B.G., 1999. Irrigation of grapevines with saline water at different growth stages. I. Effects on soil salinity and sodicity, vegetative growth and yield. Aust. J. Agric. Res. 50, 343–355.
Stevens, R.M., Ewenz, C.M., Grigson, G., Conner, S.M., 2012. Water use by an irrigated almond orchard. Irrig. Sci. 30 (3), 189–200.
Torrecillas, A., Alarcon, J.J., Domingo, R., Planes, J., Sanchez-Blanco, M.J., 1996. Strategies for drought resistance in leaves of two almond cultivars. Plant Sci. 118, 135–143.
Wang, Z., Jin, M., Šimůnek, J., van Genuchten, M. Th., 2014. Evaluation of mulched drip irrigation for cotton in arid Northwest China. Irri. Sci. 32, 15–27.
Ward, Frank A., Pulido-Velazquez, M., 2008. Water conservation in irrigation can increase water use. Proc. Natl. Acad. Sci. U. S. A. 105 (47), 18215–18220.
Xiao, Q., McPherson, E.G., Ustin, S.L., Grismer, M.E., Simpson, J.R., 2000. Winter rainfall interception by two mature open-grown trees in Davis, California. Hydrol. Process. 14, 763–784.